Design, Synthesis and Exploration of a New Molecular Motor

J.C.M. Kistemaker

M.G.M. Jongejans, D. Pijper, B.L. Feringa

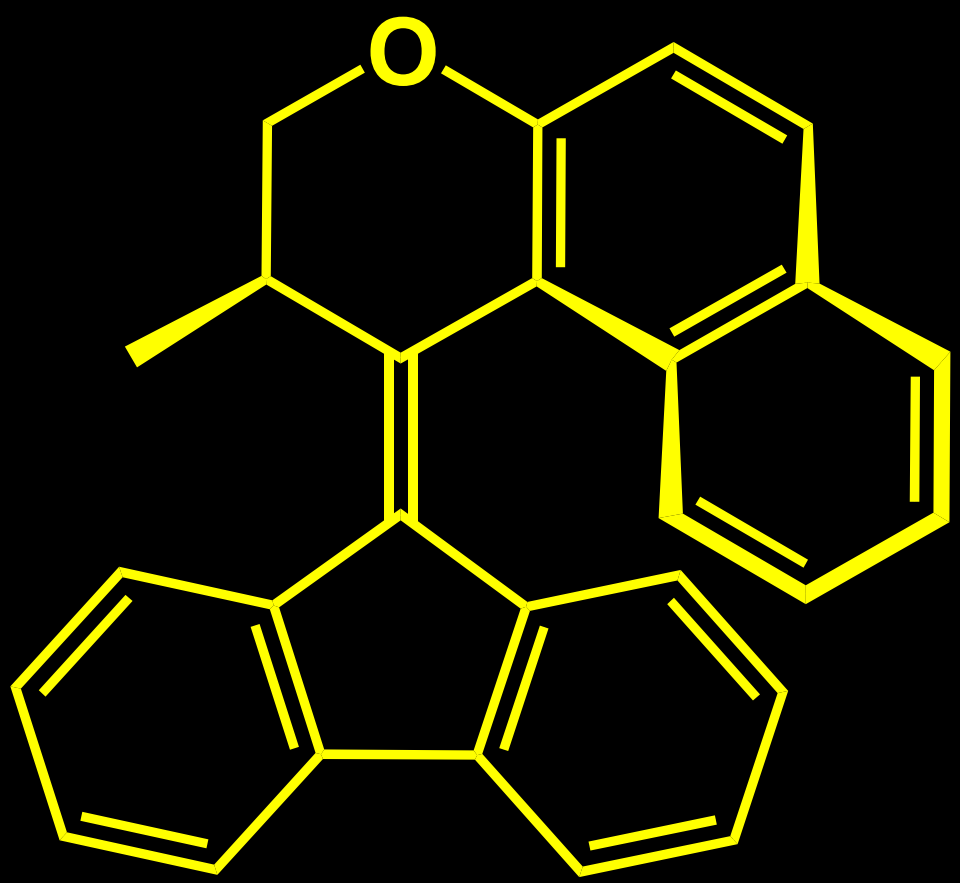

CONTENTS

1. THE MOLECULAR MOTOR

The bottom-up construction of nanosized machinery offers a magnificent challenge to chemists, and with success they synthesized propellers,[1] switches,[2] shuttles,[3] brakes,[4] turnstiles,[5] rotors,[6] ratchets,[7] and gears.[8] Building a motor, thus the controlled conversion of energy into a unidirectional rotary motion seemed difficult to achieve until Koumura, Feringa and coworkers[9] synthesized an overcrowded alkene (a biphenanthrylidene) which showed a rotation around a central carbon-carbon double bond with each 360° rotation involving four discrete isomerization steps (*fig 1*). Two light-induced cis-trans isomerizations are responsible for a 180° rotation around the central carbon-carbon double bond in which two chiral substituents govern the direction and each isomerization is followed by a thermal isomerization step involving a helix inversion where the methyl substituents adopt the more favorable axial conformation, which effectively blocks reverse rotation, and adds the four individual steps up to a single full rotation in one direction.

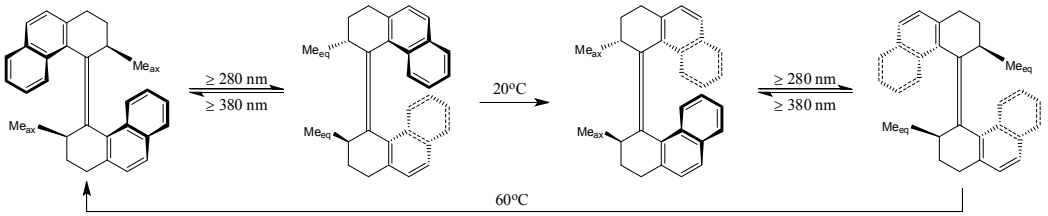

Figure 1. Full rotational cycle

The next step in the development of the motor was the distinction of upper and lower halves in the motor, for such a feature would be essential for coupling the motor to e.g. a surface. Such a second generation motor was reported by Koumura, Feringa and coworkers[10] in 2000 shown to the bottom (*fig 2*). This new type of molecular motor contains a chiral 2-methyl-2,3-dihydrothiopyran upper part and a xanthene lower part. The cycle still holds four distinct steps, but the thermal isomerization steps now have similar barriers, for the bottom half of the second generation motor is symmetrical. And due to a relief of steric hindrance in the region between the upper naphthalene and the lower phenyl moiety, named the 'fjord-region' (*fig 2*), the rotation is 10,000 times faster. The direction of rotation in the second generation motors is governed by only one stereogenic centre.

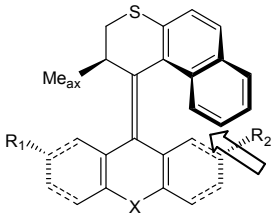

Figure 2. Fjord region

1 Iwamura, H.; Mislow, K. Acc. Chem. Res. 1988, 21, 175.

2 Feringa, B.L.; Jager, W.F.; De Lange, B.; Meijer, E.W. J. Am. Chem. Soc. 1991, 113, 5468-5470.

3 Bissel, S.A.; Córdova, E.; Kaifer, A.E.; Stoddart, J.F. Nature 1994, 369, 133-136.

4 Kelly, T.R.; Bowyer, M.C.; Bhaskar, K.V.; Beddington, D.; García, A.; Lang, F.; Kim, M.H.; Jette, M.P.J. Am. Chem. Soc. 1994, 116, 3657.

5 Bedard, T.C.; Moore, J.S. J. Am. Chem. Soc. 1995, 117, 10662-10671.

6 Schoevaars, A.M.; Kruizinga, W.; Zijlstra, R.W.J.; Veldman, L.; Spek, A.L.; Feringa, B.L. J. Org. Chem. 1997, 62, 4943.

7 Kelly, T.R.; Tellitu, I.; Sestelo, J.P. Angew. Chem. Int. Ed. 1997, 36, 1866-1868.

8 Clayden, J.; Pink, J.H.; Angew. Chem. Int. Ed. 1998, 37, 1937-1939.

9 Koumura, N.; Zijlstra, R.W.J.; van Delden, R.A.; Harada, N.; Feringa, B.L. Nature 1999, 401, 152-155.

10 Koumura, N.; Geertsema, E.M.; Meetsma, A.; Feringa, B.L. J. Am. Chem. Soc. 2000, 122, 12005-12006.

Substitution of a six-membered by a five-membered ring upper half and no bridging atom in the lower half in the second generation molecular motors resulted in a significant increase in the speed of rotation. The second generation motors with sulphur as bridging atom in the lower half and a five-membered ring upper half are reported as the fastest so far with a half-life of 10^{-9} seconds (*fig 3*).

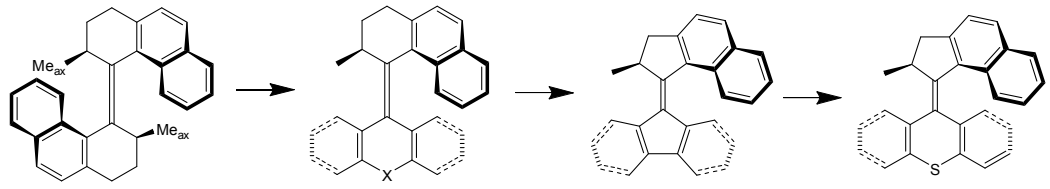

$t^{o}_{1/2}$ 439 h 39.9 m 3.17 m 10^{-9} s

Figure 3. Rotation rates

The next chapter handles a distinctive use which has been found for the motors. The molecular motors can be doped in liquid crystals upon which some of the liquid crystals can act as an amplification of the chirality of the molecular motor. When an suitable achiral liquid crystal is doped with a molecular motor, it undergoes large changes in optical properties which are characteristic for the introduced motor. A range of motors can act as such dopants.[11]

11 Eelkema, R. Thesis Liquid crystals as amplifiers of molecular chirality, 2006.

2. DOPING OF LIQUID CRYSTALS

Most substances exist in three states of matter (phases): solid (most often crystalline), liquid and vapor. The difference between these phases is the degree of order in the substance, which is directly related to its temperature and pressure. At low temperatures, when the substance is in its solid state, the atoms, ions or molecules cannot move about freely, and the constituents only movements are thermal vibrations around an equilibrium position (*fig 4,l*).
Raising of the temperature leads to a higher energy in the system which gives rise to stronger vibrations. The long range positional order is broken at the transition temperature between the solid and liquid phase and the constituents can move about in a random fashion (*fig 4,m*). But in the liquid phase the temperature is still not high enough to completely overcome the attractive forces between the constituents, so there is still some positional order at short range. Because of residual cohesion, the density of the liquid is constant even though the liquid takes the shape of its container. The liquid and solid states of matter are called condensed phases. Raising of the temperature even higher leads to such high vibrations that the substance enters the gas phase in which all positional order has been lost (*fig 4,r*).

Figure 4. States of matter

A number of organic substances possess more condensed states of matter than the basic two. The states of matter occurring between solid and liquid are called the liquid crystalline states and their constituent molecules are often called mesogens (*fig 5*). A large variety of molecules are known that possess one or more liquid crystalline phases, sometimes called mesophases. These molecules show a large diversity in form and orientation, but they all have a strongly anisotropic shape in common. Most of these molecules have a rod-like shape, but there are also disc-, bowl- and banana-shaped molecules known which form a liquid crystalline phase.
In the description above of the most common phases, only the degree of positional order was taken into account, but because of the anisotropic shape of the mesogens, the orientational order in the substance must also be considered.
The liquid crystalline states of matter exhibit a high orientational order as the solid state does, while the positional order is quite limited as in the liquid state. The positional arrangement in the liquid crystalline phase varies from complete disorder, to order in a single dimension in which it forms layers. A substance in a liquid crystalline phase is therefore a liquid in that it takes the shape of its container. The liquid is given high orientational order at the same time which endows the liquid with strongly anisotropic properties, which distinguishes it from normal liquids which are always isotropic. The liquid phase of a substance which shows liquid crystalline behavior is therefore called the isotropic phase.

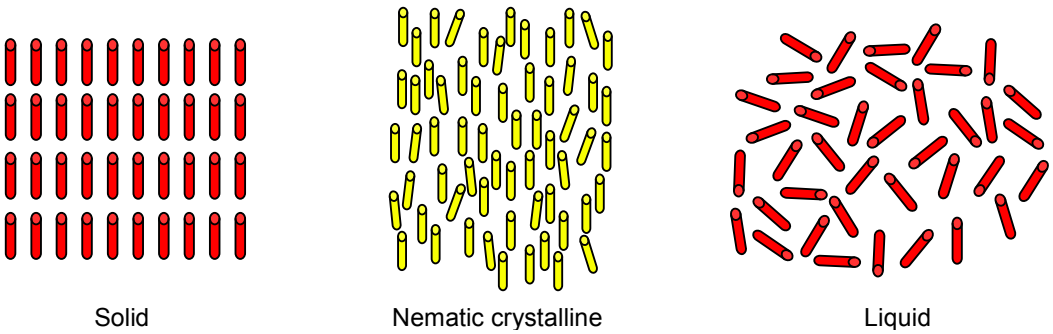

Figure 5. Condensed states of matter

The simplest liquid crystalline phase is the nematic phase (N) which is named after the Greek word νημα (nema meaning thread) for it often appears to have microscopic threads. It has a small orientational order in a single direction (*fig 5,m*).
The molecules in the nematic phase tend to be parallel to a common axis, labeled by a unit vector (director) $\hat{n}$. This means that the molecules are free to translate and rotate around their long axis but spend more time pointing in the direction of the director, than they do in any other direction. This creates a total average in a single direction providing the orientational order.
The cholesteric (or chiral nematic, N*) liquid crystalline phase, which is named after cholesterol which was the first liquid crystal that showed this behavior, has a higher degree of orientational order than the nematic phase (*fig 6*). The direction of the nematic phase stays constant while going through the sample, the cholesteric phase however changes it's direction throughout the sample in a helical shape with the director perpendicular to the helix axis. The orientation of the director goes through a helical change along the cholesteric helix axis that is non-superimposable on its mirror image, which makes it chiral. This property gives a cholesteric substance supermolecular chirality. The supermolecular chirality is characterized by its sign (P or M helix) and pitch (p), which is the distance over the cholesteric helix axis about which the director makes a 360 degree rotation. A simpler explanation of these crystalline phases might be the following. A nematic crystalline phase is build up from rod-like molecules all pointing in the same direction, just like the sticks of a game of Mikado in a box. Then the cholesteric crystalline phase in which the molecules point in the same direction but the direction changes going through the liquid crystalline phase, is the same as a lot of different games of Mikado, stacked onto each other, but the next one slightly tilted in one direction with respect to the other.

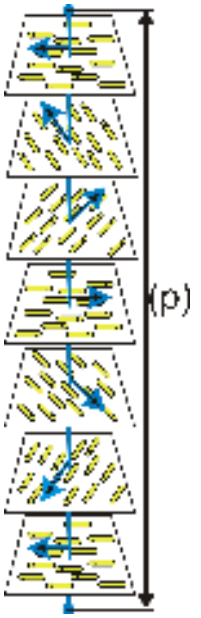

Figure 6. Cholesteric LC

There are two types of cholesteric liquid crystallinity. The first type is made up of the natural occurring mesogens which are chiral themselves and form a cholesteric liquid crystalline phase. The second type is the induced cholesteric liquid crystallinity which can be done by sandwiching nematic phase forming mesogens between two alignment layers. This gives the liquid crystalline phase the same twist as the twist of one alignment layer with respect to the other. Another way of inducing a cholesteric phase is doping a nematic crystalline phase with a chiral guest on which the mesogens assume the same chirality as the host.
Doping the liquid crystalline phase with a chiral guest, like the motor, can amplify the chirality of the dopant by tens of thousands. But the properties of the induced cholesteric phase, such as the sign and the magnitude of the cholesteric pitch, is completely dependent on the interactions between the mesogens and the host. The efficiency of a dopant to induce a helical twist in the liquid crystalline phase is described by the helical twisting power (β). The helical twisting power (HTP) is a factor which is intrinsic to every dopant - liquid crystalline combination, and it states the combination of concentration (c) and enantiomeric excess (ee) needed to obtain a cholesteric phase with a particular pitch. The pitch is inversely proportional to the concentration, HTP and enantiomeric excess of the dopant: $p = \frac{1}{c \cdot \beta \cdot ee}$.

3. NEW MOTOR DESIGN

The aim of this project was to synthesize a motor with a reasonable helical twisting power, and an intermediate barrier for the thermal isomerization. Helical twisting powers in the order of 20 μm^{-1} and higher are considered reasonable and an intermediate thermal barrier lies in the region of a half-life between an hour and several days at room temperature.

There are two simple molecular motors of which an intermediate might show the desired properties. The five-membered ring upper half motor **8** in figure 7 has a high HTP of 56 μm^{-1} and a thermal barrier with a half-life of 3.17 minutes, while the six-membered ring upper half motor **7** (fig 7) has no HTP but a thermal barrier with a half-life of 1376 years.

Previous research showed for second generation, fluorene lower half substituted motors that an increase in steric hindrance in the fjord region was correlated with an increase in the activation energy of the thermal isomerization.[12]

The aim was to increase the size of the five-membered ring, and the initial step was to use a hetero-atom of a larger size than carbon. The aim was the five-membered sulfur ring upper half, but it showed problems in previous synthesis. Instead of the desired ketone, the reaction gave the enolate form which could not be coupled to the lower half. The next step was, instead of making the five-membered ring bigger, reducing the size of the six-membered ring. The carbon on top in the six-membered ring has expected bond lengths of 1.541 to the left and 1.530 to the right carbon. If this carbon were replaced with an oxygen the bond lengths would have an expected change to 1.43 to the left and 1.36 to the right carbon.[13] These values give diameters of 2.561, 3.022 and 2.929 Å for the five-, six- and oxygen substituted six-membered ring respectively. Such a substitution would reduce the ring size, even though the C-C-C bond angle is slightly smaller than the C-O-C bond angle.

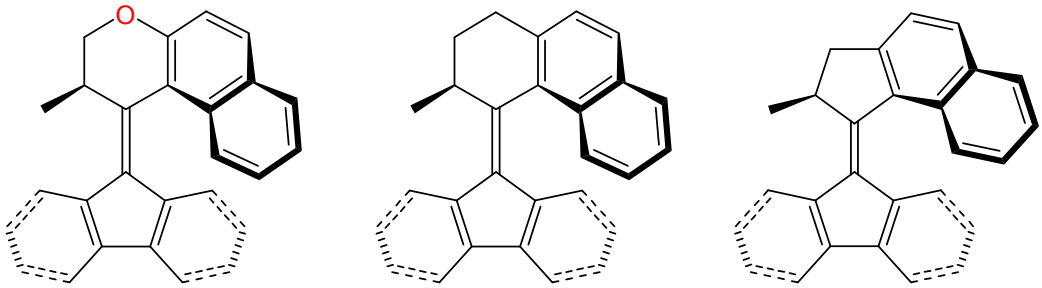

6 **7** **8**

*Figure 7. Motors **6 7 8***

[12] Vicario, J.; Meetsma, A.; Feringa, B.L. Chem. Comm. 2005, 5910-5912.
[13] Handbook of Chemistry and Physics 60th ed. 1980, F-216-F-217.

4. SYNTHESIS OF THE NEW MOTOR

The intended molecule **6** was synthesized out of naphthol in six steps with an overall yield of 11%. An alkylation with acrylonitrile gave the nitrile **1** which underwent an acidic Friedel-Crafts cyclization to form ketone **2**. Deprotonation of **2** with lithium diisopropylamide afforded the enolate which was methylated at the 2 position with methyliodide. Reflux in toluene with phosphorus sulfide gave thioketone formation which was directly applied to quick flash column chromatography. The collected fraction of thioketone was immediately added to a solution of diazofluorene in toluene and reflux over 72 hours gave a mixture of episulfide **5** and alkene **6**. Reflux with triphenylphosphine and workup with methyliodide fully converted the episulfide into the alkene. Separation of the enantiomers was achieved by preperative HPLC (chiralpak OD, heptane : 2propanol = 99.5 : 0.5).
The alkene was fully characterized by ^{1}H and ^{13}C NMR and HRMS. A chemical shift in the ^{1}H NMR for the methyl substituent in the upper half at high field of 1.45 ppm is consistent with a pseudoaxial orientation.

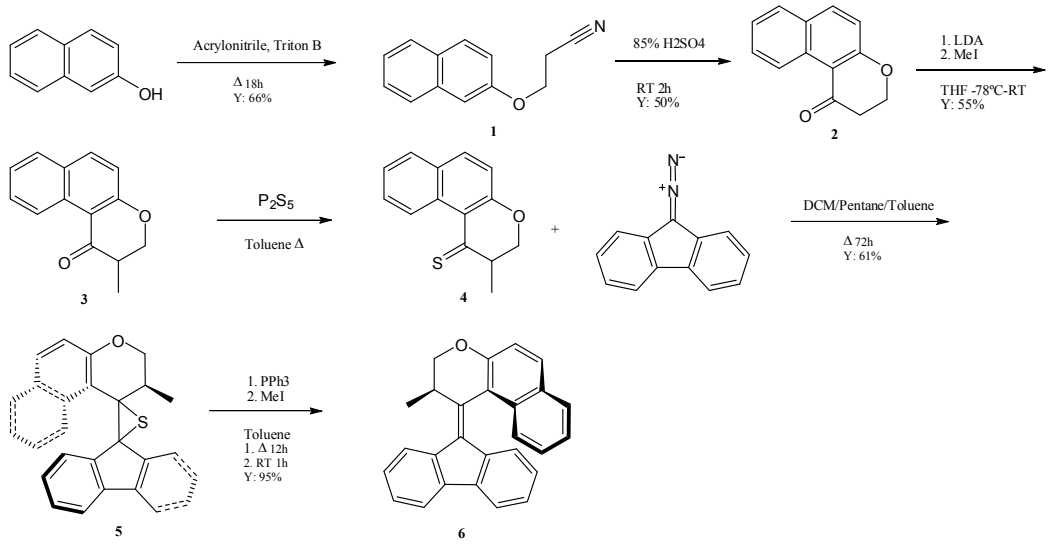

Figure 8. Synthesis

5. Exploring the Properties of the New Motor

The preferred helicity was assumed to be dependent on the stereogenic configuration of the methyl substituent and in accordance with the analogous five- and six-membered carbon ring upper half motors.[1] This led to a preferred (M)-helicity for the (R)-enantiomer and a preferred (P)-helicity for the (S)-enantiomer.

Irradiation of an NMR-sample in chloroform (365 nm) was performed at room temperature to characterize the unstable form. The downfield shift of the doublet corresponding to the methyl substituent at 1.45 ppm to 1.60 ppm confirms the pseudoaxial to pseudoequatorial conformational change (*fig 8*). An upfield shift of a doublet and a triplet at 6.72 and 6.53 to 6.48 and 6.00 ppm, respectively, corresponding to the protons on carbons 1', 2', 8' and 7', respectively, shows the rotation around the central double bond which forces the proton on carbon 8' deeper in the naphthalene moiety in the unstable form than the proton on carbon 1' in the stable form.

The photostationary state (PSS) was reached after 90 seconds and NMR indicated an excess greater than 95% of unstable form. HPLC analysis of the sample confirmed a PSS of 99:1 (unstable:stable). There was no thermal helix inversion observed within 24 hours on NMR scale.

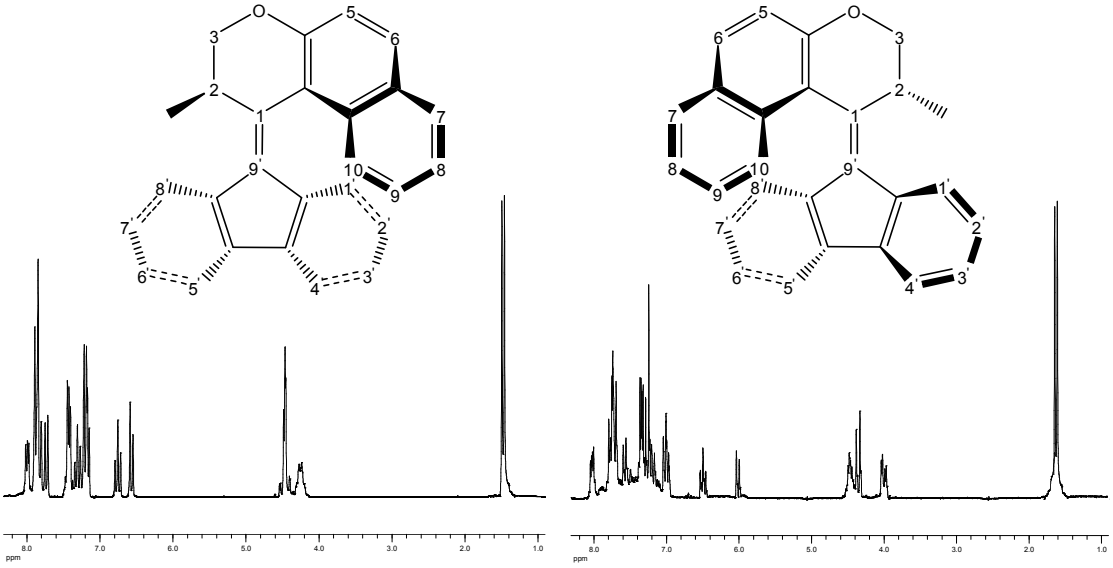

*Figure 8. NMR of stable and unstable configurations of **6***

Irradiation of a sample in dodecane (365 nm) was performed at room temperature to PSS and measured with UV (*fig 9*). The sample was left for 24 hours at room temperature and no change in the UV-spectrum was observed. This indicated the intended high thermal barrier for the helix inversion. Hereafter the sample was heated to 200°C for 5 minutes and the initial UV spectrum was regained which indicated a complete thermal helix inversion but a desymmetrization is needed to prove this unequivocally since in theory a thermal cis-trans isomerization is possible as well. An isosbestic point was found at 404 nm.

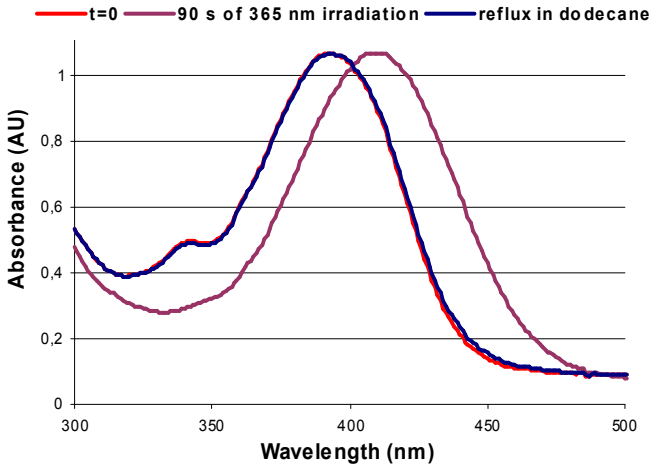

Figure 9. UV-spectra of motor 6

Due to the helical structure of the overcrowded alkene, the photochemical and thermal isomerization can be monitored by CD spectroscopy (figures 10-13). Enantiopurity was obtained by chiral HPLC as mentioned above. Irradiation of the sample in dodecane (365 nm) was performed at room temperature to PSS and a complete inversion of the CD signal was observed. Heating the sample to 200°C restored the CD-spectrum of the initial state.

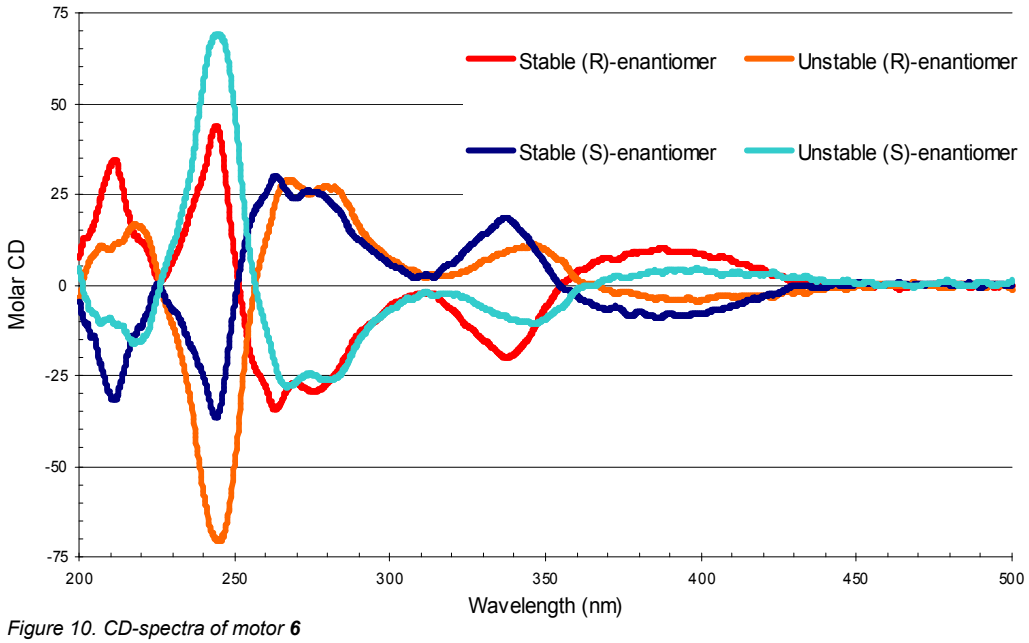

*Figure 10. CD-spectra of motor **6***

For both the stable and unstable isomers strong Cotton-effects were observed which unambiguously determined the helical configuration for the two isomers (*fig 10*). The second fraction from the HPLC was obtained in 100% ee and appeared to be the (R)-enantiomer, the first fraction was obtained in 93% ee and appeared to be the (S)-enantiomer. In further experiments only the pure (R)-enantiomer was used.

A sample of (R)-alkene with (M)-helicity in dodecane was prepared and irradiated in the CD-spectrometer at several temperatures to its photostationary state. The change in the intensity of the CD band at 244 nm was measured over time to allow the monitoring of the rate of conversion of the unstable isomer. Consequently the rate constant (k) at different temperatures was acquired, corresponding to a first order kinetic process. Calculation of the enthalpy of activation ($\Delta H^{\ddagger}$), entropy of activation ($\Delta S^{\ddagger}$) and the Gibbs free energy of activation ($\Delta^{\ddagger}G^{o}$) can be obtained from an Eyring plot (*fig 11*). With these figures the rate constant (k^{o}) and the half life ($t^{0}_{1/2}$) at room temperature can be determined. The results are summarized in table 1 together with the results for the five- and six-memberedring alkenes **7** and **8**.

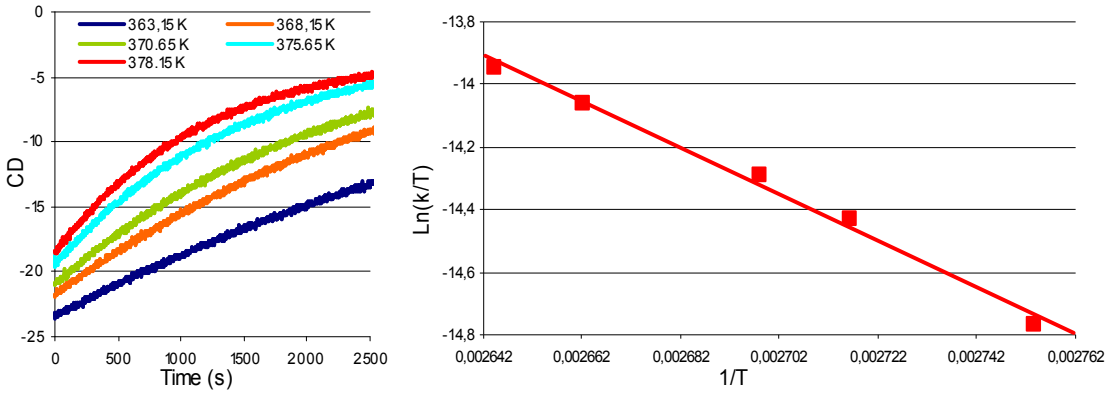

*Figure 11. CD-spectra of isomerization at different temperatures (left), Eyring plot for motor **6** (right)*

Motor	PSS (unstable : stable)	k^0 (s^{-1})	$\Delta^{\ddagger}G^{o}$ (kJ mol^{-1})	$t^0_{1/2}$ (h)
6	99 : 1	8.76×10^{-7}	106	220
7	91 : 9	1.60×10^{-11}	139	1.21×10^{8}
8	75 : 25	3.64×10^{-3}	85	5.28×10^{-2}

*Table 1. Comparison of the properties of motors **6**, **7** and **8***

The first demand of the desired overcrowded alkene **6** has been met, for the motor shows an intermediate thermal barrier with a half-life of 9.2 days at room temperature. Such a half-life makes it feasible to apply the molecular motor as a stable switch at room temperature. The first photochemical cis-trans isomerization at 365 nm yields the 'unstable' isomer in which the methyl substituent takes the less stable equatorial position with a PSS of 99 : 1 (*fig 12*). A second photochemical cis-trans isomerization takes place at 475 nm which yields the 'stable' isomer with the methyl substituent in the favorable axial position with a PSS of 99 : 1 resolved by HPLC. This characteristic switching property was put to the test with CD-measurements in which the 'motor' was switched back and forth 8 times (*fig 13*). Irradiation times of 10 minutes for the cis-trans isomerization at 365 and 2 hours for the cis-trans isomerization at 475 nm were employed. After each cycle the initial CD spectrum was retrieved and photostationary states were above 99% according to CD.

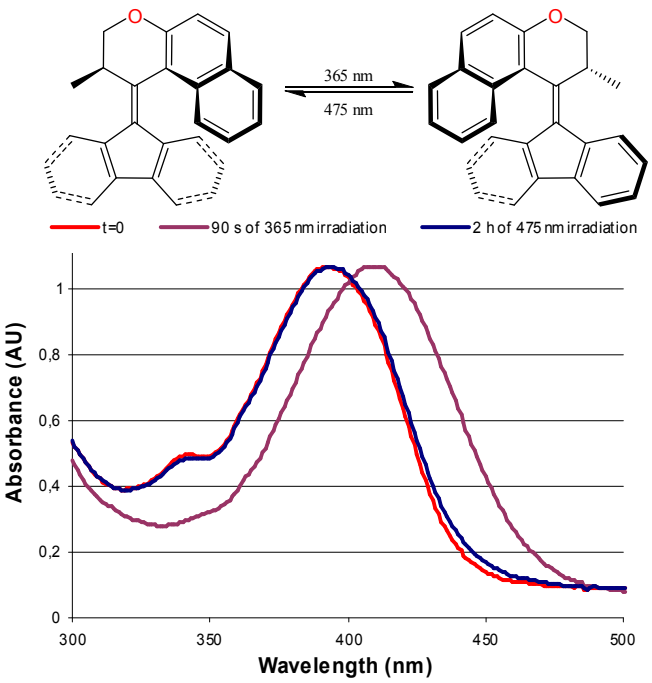

*Figure 12. Reactions scheme and UV-spectrum of switching motor **6***

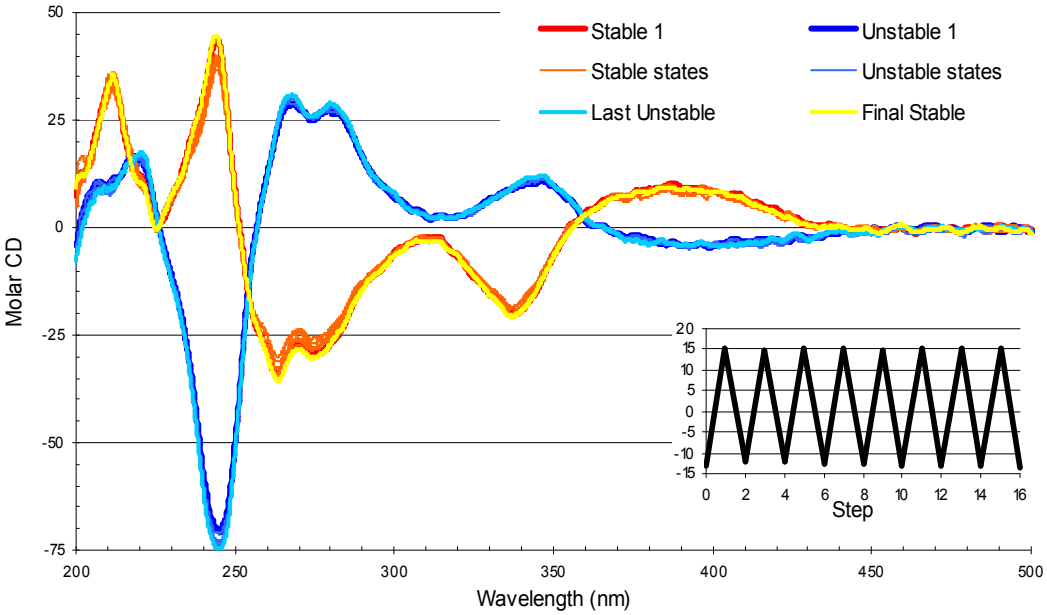

*Figure 13. CD-spectra of 8 cycles of switching motor **6***

6. Doping of the New Motor in a Liquid Crystal

The enantiopure molecular motor (2R)-(M)-**6a** was doped in different concentrations in nematic liquid crystals in order to obtain a cholesteric liquid crystalline phase. At a concentration of 1 weight percentage of molecular motor with respect to liquid crystal E7 a decent cholesteric liquid crystalline phase was obtained with the cholesteric helix axis parallel to the surface of the glass slide providing the desired 'fingerprint' texture (*fig 14*). The sample was then irradiated (365 nm) and followed in time (*fig 15*). The fingerprint broadened until it completely disappeared, giving a nematic phase after approximately 50 seconds. After 90 seconds the lines appeared again and contracted over time. After 270 seconds of irradiation no changes were observed, acting in accordance with the observations made by circular dichroism under irradiation.

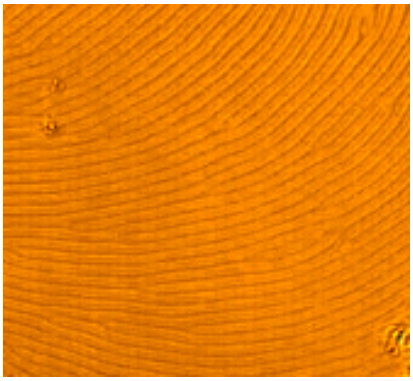

*Figure 14. LC doped with motor **6***

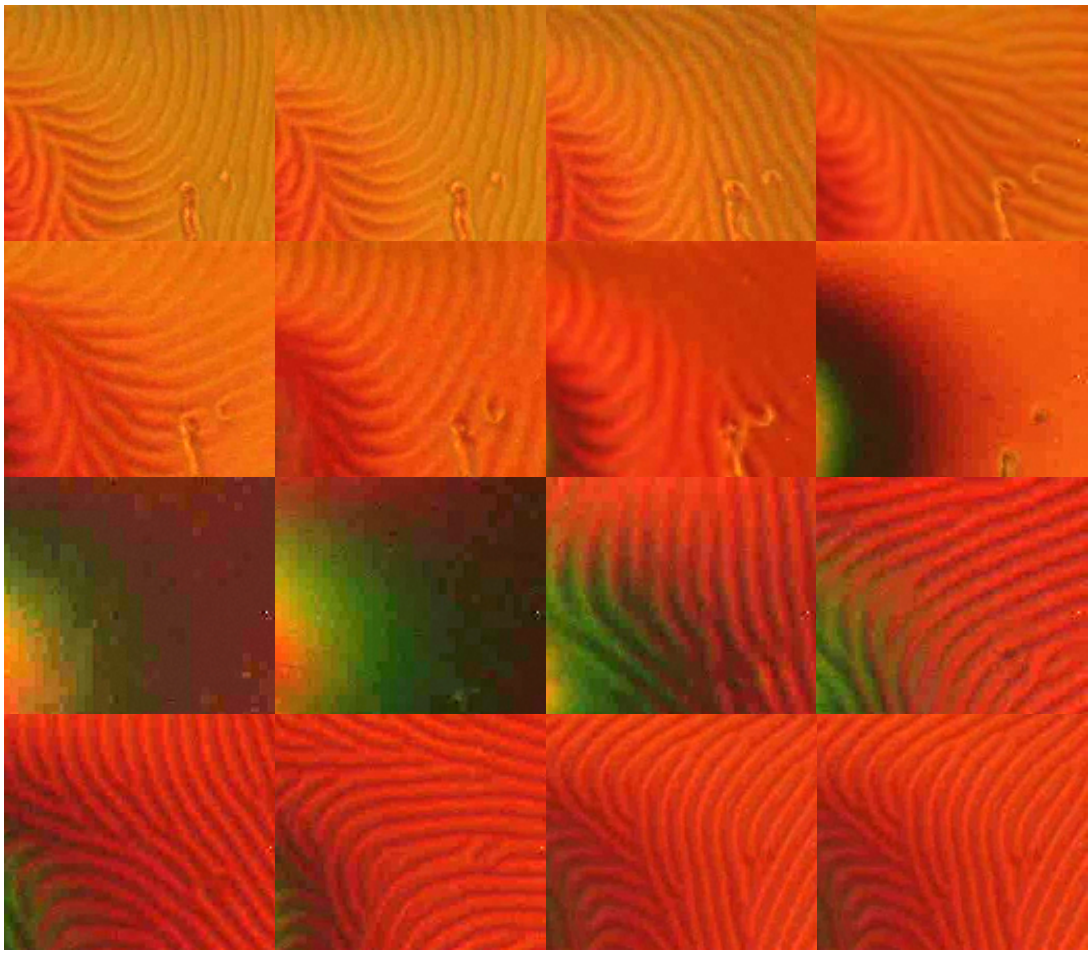

*Figure 15. Irradiation of the LC doped with motor **6***

It was found that the fingerprint texture reorganized in a rotational manner during irradiation. Going from the (2R)-(M)-**6a** doped cholesteric phase to a nematic state of matter under irradiation the line texture rotated counterclockwise, while going from the nematic phase to the (2R)-(P)-**6b** doped cholesteric phase the line texture rotated clockwise. The opposite phenomenon was observed for the (2S)-(P)-**6a** doped cholesteric phase for which the fingerprint rotated clockwise upon irradiation until it reached a nematic phase and counterclockwise going from the nematic phase to the (2S)-(M)-**6b** doped cholesteric phase. These findings are consistent with previous research[14].

14Eelkema, R.; Pollard, M.M.; Vicario, J.; Katsonis, N.; Ramon, B.S.; Bastiaansen, C.W.M.; Broer, D.J.; Feringa, B.L. Nature 2006, 440, 163.

A lens of known radius was applied to (2R)-(M)-**6a** doped liquid crystalline films with known concentrations in order to determine the helical twisting power of the stable and unstable form of the molecular motor. Grandjean-Cano lines were observed and the pitches were determined indirectly by measuring the distances between consecutive lines (*fig 16*). Helical twisting powers of -31 ± 4 μm^{-1} for stable (2R)-(M)-**6a** and 33 ± 2 μm^{-1} for unstable (2R)-(P)-**6b** at PSS were found. In table 2 the helical twisting powers of several motors are reported together with the newly found dopant. Although the HTP of (2R)-(M)-**6a** is not exceptionally large, it is definitely a reasonable HTP and as anticipated in between the HTP of motors **7** and **8**.

Molecular Motor	HTP (μm^{-1})	HTP at PSS (μm^{-1})
(2R)-(M)-**6a**. X=O, R=Methyl, Y= -	-31	33
7. X=CH_2, R=Methyl, Y=-	0	0
(2'R)-(P)-**8**. X=-, R=Methyl, Y=-	55	-22
(2'R)-(P)-**9**. X=-, R=Isopropyl, Y=-	43	-32
(2'R)-(P)-**10**. X=-, R=Tertbutyl, Y=-	6	0
(2'R)-(P)-**11**. X=-, R=Phenyl, Y=-	90	-59
(2'S)-(M)-**12**. X=-, R=Methyl, Y=O	-37	0

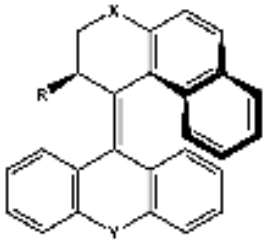

Table 2. Helical twisting powers of different motors[15]

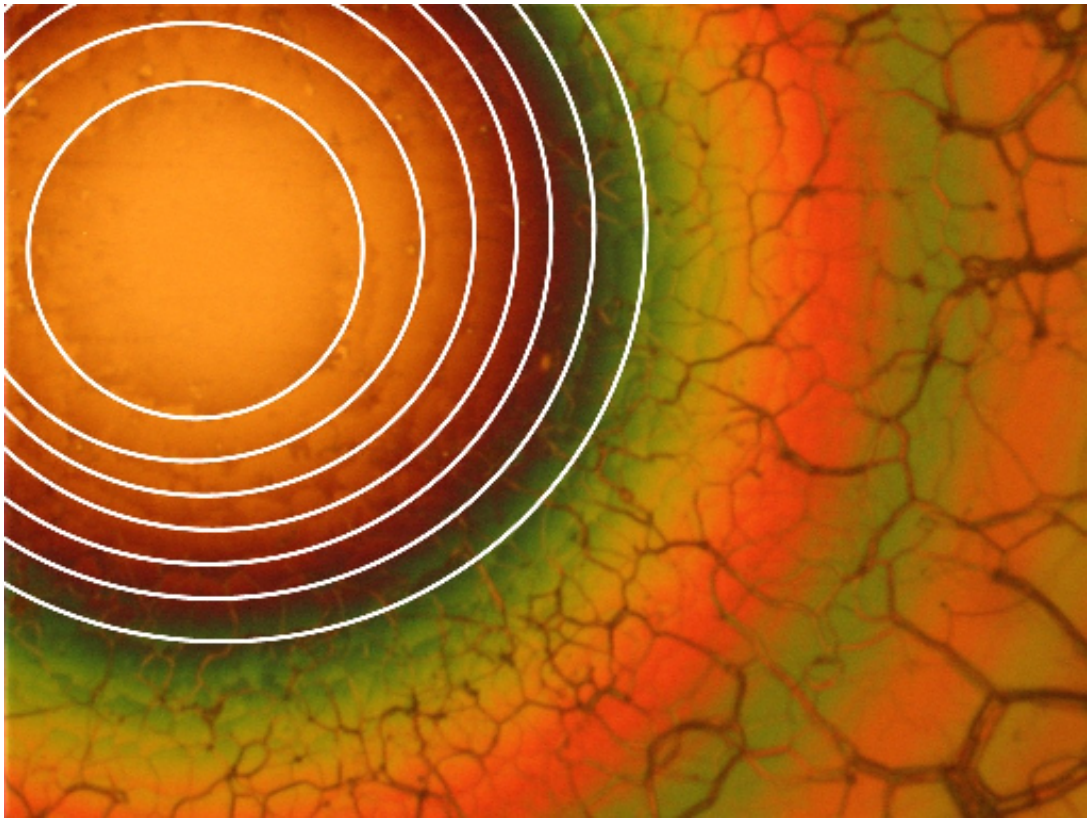

*Figure 16. LC doped with motor **6a** with a lens applied, Grandjean-Cano lines marked white*

15 Eelkema, R. Thesis Liquid crystals as amplifiers of molecular chirality, 2006.

7. GOING BACK, FROM MOTOR TO SWITCH

The first reported chiroptical molecular switch by Feringa et *al*. seems to have a lot in common with the second generation motor with the exception that it is missing a chiral substituent.[16] Since the discovery of this molecular switch, a lot of analogous molecular switches have been synthesized, as well as their corresponding chirally substituted molecular motors. A lot of these switches showed a capacity to induce a helical twist in nematic liquid crystalline phases, but the molecular switches corresponding to the molecular motors which are able to induce a cholesteric phase were not able to do this. The main reason for their inability to induce a cholesteric phase is their low thermal barrier, for they racimize at room temperature.

The height of the thermal barrier for helix inversion of the synthesized motor **6** is sufficient to prevent isomerization at room temperature. This feature might also be present in the analogous molecular switch as well as the power to generate a cholesteric phase. This molecular switch **13** was synthesized by Dr. B. de Lange[17] (figure 3, left motor without the chiral methyls substituents). Separation of the enantiomers was achieved by preparative HPLC (chiralpak OD, heptane : 2propanol = 97 : 3).

The alkene was fully characterized by ^{1}H and ^{13}C NMR and HRMS. As expected the UV spectrum did not change upon irradiation for the switch is symmetrical thus (M)-**13** and (P)-**13** give the same UV spectrum. A clear change in CD spectrum was seen upon irradiation. Within 2 minutes the enantiopure (P)-**13** sample completely racemized and the CD signal disappeared (*fig 17*).

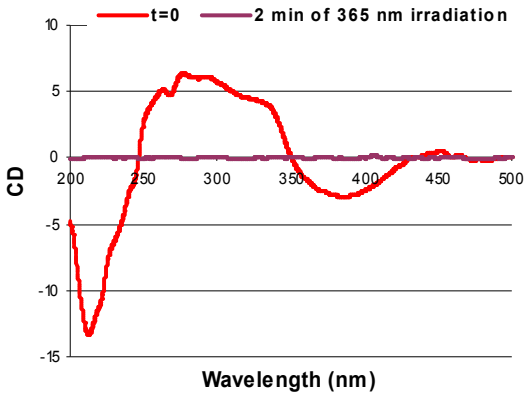

*Figure 17. UV-spectra of switch **13***

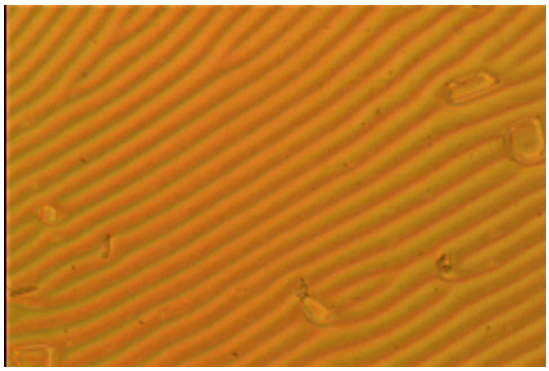

*Figure 18. LC doped with switch **13***

The enantiopure molecular switch (P)-**13** was doped in different concentrations in nematic liquid crystal E7 in order to obtain a cholesteric liquid crystalline phase. At a concentration of 0.5 weight percentage of molecular motor with respect to the liquid crystal E7 a satisfactory cholesteric liquid crystalline phase was obtained with the cholesteric helix axis parallel to the surface of the glass slide providing the desired 'fingerprint' texture (*fig 18*). The sample was then irradiated (365 nm) and followed in time (*fig 19*). The fingerprint broadened until it completely disappeared, giving a nematic phase after approximately 45 seconds.

The same phenomenon was observed as was with the molecular motors since P-helical motors gave clockwise rotation, so did this P-helical molecular switch.

The Grandjean-Cano technique was applied to determine the helical twisting power of molecular switch (P)-**13** (*fig 20*). The pitches were measured and a HTP of 26 $\pm$ 3 μm^{-1} was determined. This helical twisting power is relatively close to the HTP of 31 $\pm$ 4 μm^{-1} of its corresponding molecular motor **6** but shows the delicate host-guest interplay in doping of nematic liquid crystalline phases. The removal of a methyl already reduces the HTP with 5 μm^{-1}, the substitution of a carbon atom for an oxygen suddenly brings the HTP from 0 to 31 μm^{-1} and reducing a six-membered ring to a five-membered ring upper half brings the HTP from 0 to 55 μm^{-1} (*table 3*). It appears that a trend might be hard to find if such small changes bring about such large differences in helical twisting power and such large errors (relative errors ranging from 7 to 13 %).

16 Feringa, B. L.; Jager, W. F.; De Lange, B.; Meijer, E. W. J. Am. Chem. Soc. 1991, 113, 5468-5470

17 Thesis Ben de Lange

Molecular Motors	HTP (μm^{-1})	HTP at PSS (μm^{-1})
7. X=CH_2, R=Methyl, Y=-	0	0
(P)-**13**. X=O, R=H, Y= -	26	-
(2R)-(M)-**6a**. X=O, R=Methyl, Y= -	-31	33
(2'R)-(P)-**8**. X=-, R=Methyl, Y=-	55	-22

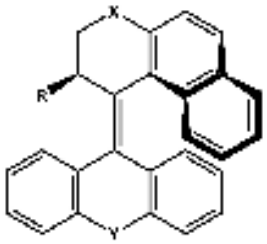

Table 3. Helical twisting powers of different compounds[18]

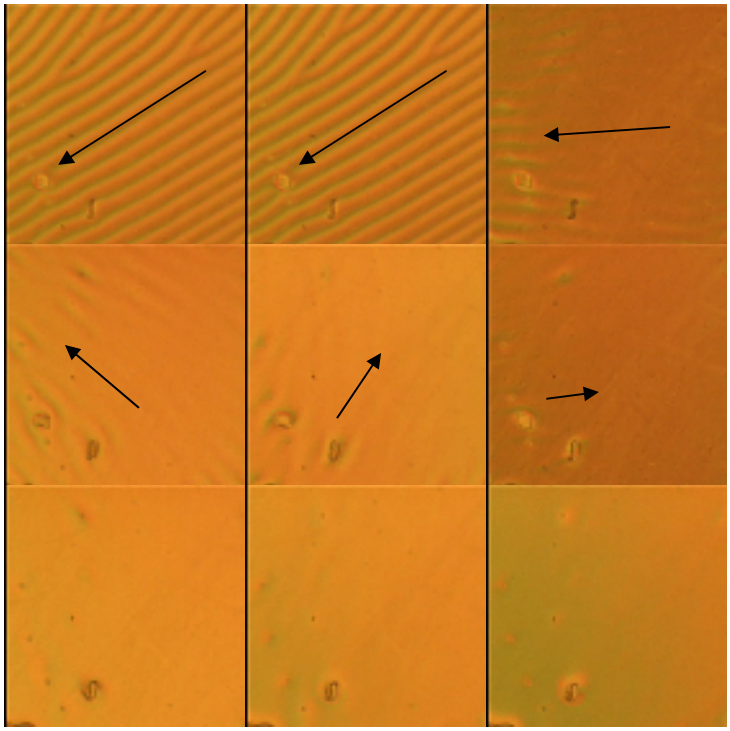

*Figure 19. Irradiation of an LC doped with switch **13***

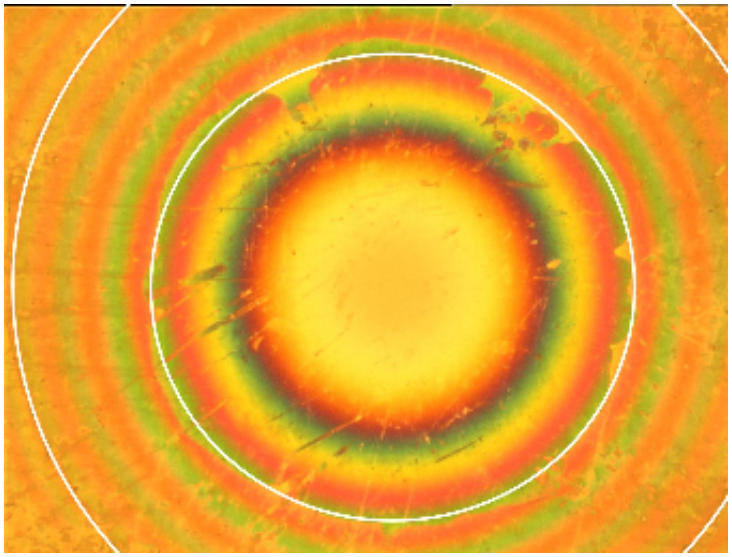

*Figure 20. LC doped with switch **13** with a lens applied, Grandjean-Cano lines marked blue*

18 Eelkema, R. Thesis Liquid crystals as amplifiers of molecular chirality, 2006.

8. VORTICES

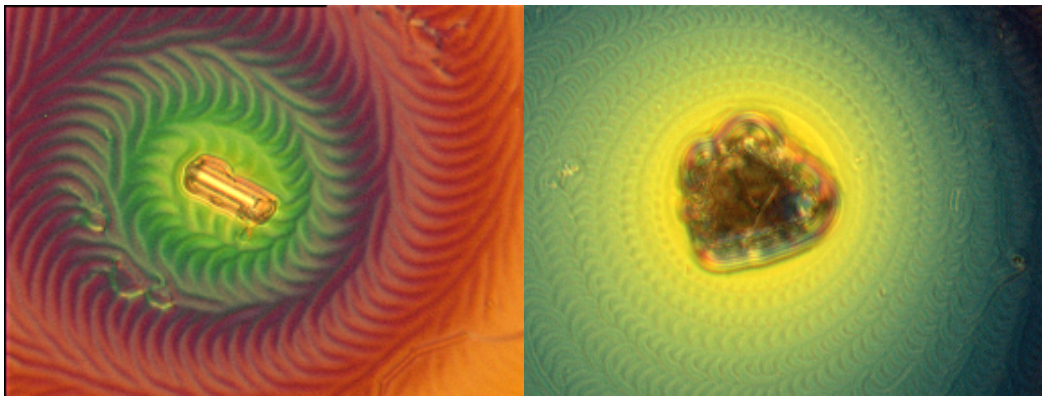

*Figure 21. Liquid crystalline phases doped with molecular motor **11**. Interspersed with glass rods (r=30μm) (left), interspersed with saltparticles (right), one shown of each, 20x enlarged.*

Figure 22. Animated motivation for theory on increase in number of rotations and so decrease in widths of the single bands[18]

During the observations of the rotational effect of the liquid crystalline phase on small objects such as glass rods placed on it, a strange phenomenon was noticed (*fig 21*). When the glass rod was too heavy to drift on the liquid crystalline phase it sunk into it forming a pattern similar to a snails shell, later called a vortex. Different objects such as sodium chloride crystals, silica particles and magnesium sulfate gave a similar result, only differing in width of the single bands. Larger objects gave smaller widths, were small objects gave large widths, possibly due to adhesion effects, the solvent forms a bulge around the object. Hence, the larger the object, the higher the bulge, as illustrated in figure 21. This would give less space for the same amount of rotations which leads to a smaller width of a single rotation. AFM should be able to prove this theory.[19]

At irradiation of the liquid crystalline phase the vortex spiraled inwards, slowly disappearing from the outside (*fig 22*). It took the cholesteric phase the same amount of time as usual to reach the nematic phase. Further irradiation made a vortex of opposite helicity spiral outwards and slowly a cholesteric phase was formed again. The most striking feature of these vortices is the inverting helicity on irradiation. And the same occurrence was observed going through the thermal isomerization. When the liquid crystal was doped with the motors enantiomer the opposite effect was seen upon the introduction of similar glass rods. A vortex with opposite helicity was formed around the glass rod and upon radiation the helicity of the vortex also inverted.

The liquid crystalline phase doped with the switch showed a vortex as well although it had a significant larger width using the same glass rods. The helicity was consistent with the intrinsic helicity of the molecule with which the liquid crystalline phase was doped. At the time of writing, these vortices are explored further for consistency with the other molecular motor doped crystalline phases and cholesteric phases doped with random chiral molecules.

19 Bouligand, Y. Le Journal de Physique 1972, 33, 715-736.

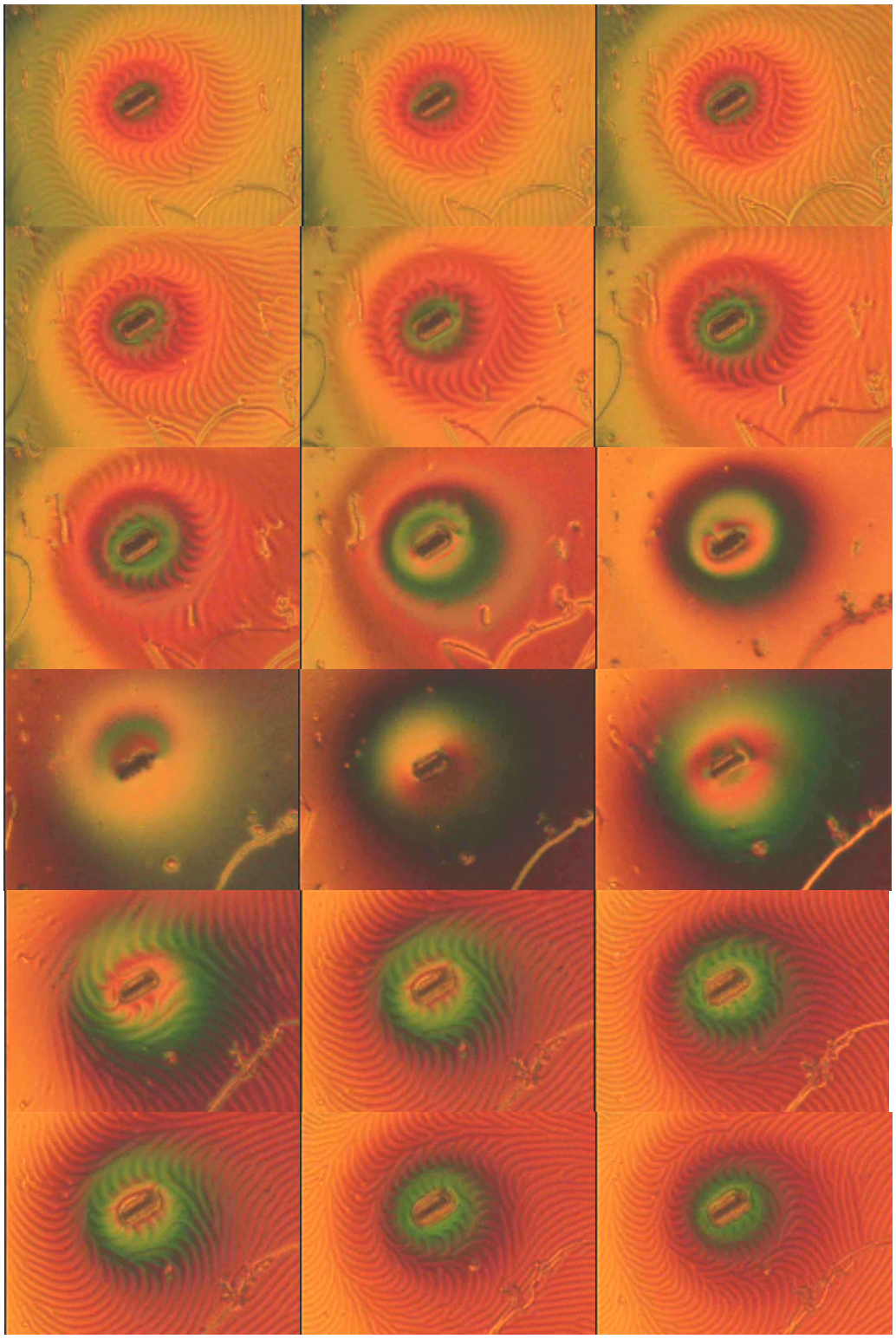

*Figure 23. LC doped with motor **6**, interspersed with glass rods, one shown, irradiated and 20x enlarged.*

9. EXPERIMENTAL

General remarks
Reagents were purchased from Aldrich, Merck or Fluka and were used as provided unless otherwise stated. All solvents were reagent grade and were dried and distilled before use according to standard procedures. Chromatography: silica gel, Merck type 9385 230-400 mesh, TLC: silica gel 60, Merck, 0.25 mm. Mass spectra (HRMS) were recorded on an AEI MS-902. ^{1}H and ^{13}C NMR spectra were recorded on a Varian Gemini-200 operating at 200.55 MHz for the ^{1}H nucleus, and at 50.44 MHz for the ^{13}C nucleus, in $CDCl_3$, unless stated otherwise. Chemical shift values are denoted in δ values (ppm) relative to residual solvent peaks ($CHCl_3$, ^{1}H δ=7.26, ^{13}C δ=77.0 ppm). HPLC analyses were performed on a Shimadzu 10AD-VP using a chiral OD column. A preparative Gilson HPLC system consisting of a 231XL sampling injector, a 306 (10SC) pump, an 811C dynamic mixer, an 805 manometric module, with a 119 UV-VIS detector and a 202 fraction collector, and a chiral OD column were used to separate the isomers.

Preparation of liquid crystalline films
General remarks: all solvents were HPLC or spectroscopic grade, and were used as received. The liquid crystalline material E7 was purchased from Merck, Darmstadt. A carefully cleaned microscope slide was spincoated with a commercially available polyimide (Optmer AL1051, JSR, Belgium) and allowed to harden overnight in a vacuum oven (170°C, 200 mbar). Rubbing of the surface with a polyester fabric generated a parallel alignment in the polyimide surface. Mixtures of solutions of dopants in toluene and E7 in toluene were made and applied on a unidirectionally rubbed polyimide-coated glass slide and put under the microscope. Evaporation of toluene allowed the formation of the liquid crystalline phase. Images of the LC films were recorded in transmission using an Olympus BX 60 microscope, equipped with crossed polarizers and a Sony 3CCD DXC 950P digital camera, attached to a personal computer with Matrox Inspector 2.1 imaging software.

General procedure for determination of the cholesteric pitch
The pitches of the liquid crystalline (LC) phases were determined by the Grandjean-Cano technique, using a plane-convex lens with a radius of 25.119 mm, Linos Components; Radiometer), and the optical microscope as described above. LC films were prepared as described above, and the plane-convex lens was applied. Grandjean-Cano lines could be observed, and the pitch could be determined indirectly by measuring the distances between the consecutive lines. The sign of the helical pitch was determined by CD-measurements.

CD and UV measurements
CD spectra were recorded on a JASCO J-715 spectropolarimeter using UVASOL grade hexane and dodecane (Merck) in a 1.0-mm quartz cell at ambient temperature (20-25ºC) and elevated temperatures (25-100^{o}C). UV spectra were recorded on a Hewlett-Packard HP 8453 FT spectrophotometer, using the same conditions as stated for the CD measurements.

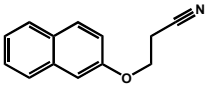

3-(naphthalen-2-yloxy)propanenitrile (1). To a solution of 2-naphthol (23.8 g, 165 mmol) in acrylonitrile (45 g, 848 mmol) Triton B (2.7 ml, 6.1 mmol) was added and stirred for 18 h under reflux. The reaction mixture was then cooled to 0 ^{o}C and filtered. The residue was washed with 5% sodiumhydroxide (75 ml) and water (40 ml) and dried affording 21.5 g (109 mmol, 66%) of nitrile **1**. ^{1}H NMR (200 MHz, $CDCl_3$) δ 7.79 (d, J=7.9 Hz, 1H), 7.77 (d, J=8.8, 1H), 7.74 (d, J=8.2 Hz, 1H), 7.46 (t, J=7.3 Hz, 1H), 7.37 (t, J=7.5 Hz, 1H), 7.17 (dd, J=2.4 , 8.9 Hz, 1H), 7.12 (d, J=2.1 Hz, 1H), 4.31 (t, J=6.4 Hz, 2H), 2.89 (t, J=6.4 Hz, 2H); ^{13}C NMR (50 MHz, $CCHCl_3$) δ 155.5 (C), 134.1 (C), 129.6 (CH), 129.2 (C), 127.6 (CH), 126.7 (CH), 126.5 (CH), 124.0 (CH), 118.4 (CH), 117.2 (C), 106.9 (CH), 62.4 (CH_2), 18.4 (CH_2).

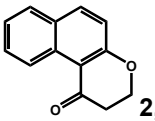

2,3-dihydro-1H-benzo[f]chromen-1-one (2). Nitrile **1** (42.1 g, 213 mmol) was added to 85% H_2SO_4 (425 ml) in 15 min and stirred for 2 h. The reaction mixture turned from yellow to red. The mixture was then poured on 1 kg ice and after melting a solid was filtered off. The liquid mixture was extracted with ether (2x 150 ml) and ethylacetate (2x 150 ml). The solvents were removed under reduced pressure and the combined solids were washed with saturated $NaHCO_3$ (300 ml) and water (250 ml). Drying afforded 21.1 g (106 mmol, 50%) of ketone **2**. ^{1}H NMR (200 MHz, $CDCl_3$) δ 9.47 (d, J=8.7 Hz, 1H) 7.85 (d, J=9.0 Hz, 1H), 7.70 (d, J=8.0 Hz, 1H), 7.62 (t, J=7.8 Hz, 1H), 7.40 (t, J=7.5 Hz, 1H), 7.05 (d, J=9.0 Hz, 1H), 4.56 (t, J=6.6 Hz, 2H), 2.87 (t, J=6.6 Hz, 2H).

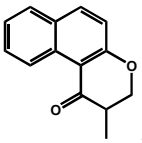

2-methyl-2,3-dihydro-1H-benzo[f]chromen-1-one (3). *n*-Butyllithium (6.25 ml, 10 mmol) was added to a stirred mixture of diisopropylamide (1.4 ml, 10 mmol) in THF (50 ml) at -78 ^{o}C. To this yellow mixture ketone **2** (2.0 g, 10 mmol) in THF (50 ml) was added dropwise in 15 min. Methyliodide (25 ml, 0.3 mol) was added and the color turned to red. The mixture was allowed to warm to room temperature and stirred overnight. The yellow mixture was poured on a saturated NH_4Cl solution (300 ml) and extracted with ethylacetate (3x 150 ml). The combined organic layers were washed with brine, dried over $NaSO_4$ and the solvent was removed under reduced pressure affording 1.17 g (5,5 mmol, 55%) of ketone **3**. ^{1}H NMR (200 MHz, $CDCl_3$) δ 9.48 (d, J=8.7 Hz, 1H), 7.91 (d, J=9.0, 1H), 7.75 (d, J=8.8 Hz, 1H), 7.63 (ddd, J=1.5 , 7.0 , 8.6 Hz, 1H), 7.42 (ddd, J=1.1 , 6.9 , 8.0 Hz, 1H), 7.09 (d, J=9.0 Hz, 1H), 4.60 (dd, J=5.1 , 11.2 Hz, 1H), 4.27 (dd, J=10.0 , 11.7 Hz,1H), 2.94 (dqd, J=5.1 , 7.0 , 10.6 Hz, 1H), 1.28 (d, J=7.0 Hz, 3H); ^{13}C NMR (50 MHz, $CCHCl_3$) δ 196.0 (C), 163.5 (C), 137.2 (CH), 131.7 (C), 129.5 (CH), 129.2 (C,C), 128.3 (CH), 125.8 (CH), 124.7 (CH), 118.6 (CH), 111.9 (C), 72.1 (CH_2), 41.2 (CH), 11.3 (CH_3).

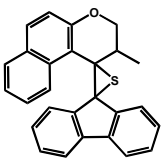

Dispiro[2,3-dihydro-2-methyl-1*H*-naphto[2,1-b]-pyran-1,2'-thiirane-3',9'-(9'H-fluorene)] (5). Under an atmosphere of nitrogen ketone **3** (1.1 g, 5.2 mmol) and P_2S_5 (10 g, 22.5 mmol) in toluene (140 ml) were heated to 70 ^{o}C until the conversion of ketone **3** into thioketone was complete (TLC, silica, pentane/DCM 2/1, $R_{f,ketone}$=0.3, $R_{f,thioketone}$=0.8). The hot solution was filtered and the green filtrate was directly applied to quick flash column chromatography (silica, pentane/DCM 2/1). The collected fraction of thioketone was immediately added to a solution of 9-diazo-9H-fluorene (3.0 g, 15.6 mmol) in toluene (140 ml) and the reaction mixture was refluxed for 72 h. The solvents were removed under reduced pressure and the residue was purified by column chromatography (silica, pentane/DCM 10/1 → 1/2) affording 1.25 g (3.17 mmol, 61%) of episulfide **5**. ^{1}H NMR (200 MHz, $CDCl_3$) δ 9.21 (d, J=8.8 Hz, 1H), 7.79 (t, J=7.7 Hz, 2H) 7.66-7.55 (m, 4H), 7.43 (ddt, J=1.2 , 3.1 , 7.4 Hz, 2H), 7.31 (dt, J=1.2 , 7.5 Hz, 1H), 7.07 (dt, J=1.0 , 7.5 Hz, 1H), 6.77 (d, J=8.8 Hz, 1H), 6.49 (dt, J=1.1 , 7.6 Hz, 1H), 6.06 (td, J=0.8 , 7.8 Hz, 1H), 3.64 (m, 2H), 3.16 (m, 1H), 1.17 (CH, J=6.9 Hz, 3H); ^{13}C NMR (50 MHz, $CCHCl_3$) δ 155.20 (C), 143.27 (C), 143.16 (C), 141.93 (C), 139.97 (C), 134.38 (C,C), 129.45 (CH), 129.33 (C,C), 128.80 (CH), 128.29 (CH), 127.46 (CH), 126.35 (CH), 126.01 (CH), 124.09(CH), 123.50 (CH), 123.25 (CH), 122.55 (CH), 120.46 (CH, CH), 119.35 (CH), 118.09 (CH), 117.65 (C), 72.44 (CH_2), 40.09 (CH), 19.19 (CH_3); HRMS (EI): calcd for $C_{27}H_{20}OS$, 392.12349; found, 392.12448.

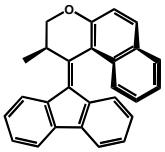

1-(9H-fluoren-9-ylidene)-2-methyl-2,3-dihydro-1H-benzo[f]chromene (6). Under an atmosphere of nitrogen episulfide **5** (1.2 g, 3.1 mmol) and PPh_3 (2 g, 7.6 mmol) in toluene (200 ml) were refluxed overnight. The mixture was allowed to cool to room temperature and after addition of MeI (50 ml) it was stirred for 1 h. Filtration and removal of the solvent under reduced pressure gave a yellow oil which was purified by column chromatography (silica, pentane/DCM 10/1) affording 1.0 g (2.9 mmol, 95%) of motor **6**. ^{1}H NMR (200 MHz, $CDCl_3$) δ 8.01-7.91 (m, 1H), 7.90-7.75 (m, 4H), 7.70 (d, J=7.6 Hz, 1H), 7.45-7.33 (m, 2H), 7.28 (dt, J=0.9 , 7.4 Hz, 1H), 7.10-7.20 (m, 3H), 6.72 (dt, J=0.7 , 7.6 Hz, 1H), 6.53 (d, J=8.0 Hz, 1H), 4.43 (m, 2H), 4.22 (m, 1H), 1.45 (d, J=7.0 Hz, 3H); ^{13}C NMR (50 MHz, $CDCl_3$) δ 153.4 (C), 140.6 (C), 139.5 (C), 138.3 (C), 137.9 (C,C), 132.6 (C), 131.9 (C), 131.8 (CH), 129.0 (C), 128.3 (CH), 127.3 (CH), 127.1 (CH), 127.0 (CH), 126.8 (CH), 126.5 (CH), 125.2 (CH), 125.0 (CH), 124.4 (CH), 123.5 (CH), 119.9 (CH), 118.9 (CH), 118.1 (CH), 113.7 (C), 72.3 (CH_2), 33.0 (CH), 15.8 (CH_3); HRMS (EI): calcd for $C_{27}H_{20}O$, 360.15141; found, 360.15025.